



HAL
open science

(Zr/Ti) ratio effect on RF magnetron sputtered lead titanate zirconate films

Caroline Soyer, T. Haccart, Eric Cattan, Denis Remiens

► **To cite this version:**

Caroline Soyer, T. Haccart, Eric Cattan, Denis Remiens. (Zr/Ti) ratio effect on RF magnetron sputtered lead titanate zirconate films. *Integrated Ferroelectrics*, 2001, 35 (1-4), pp.229-238. 10.1080/10584580108016904 . hal-00152474

HAL Id: hal-00152474

<https://hal.science/hal-00152474>

Submitted on 19 Aug 2022

HAL is a multi-disciplinary open access archive for the deposit and dissemination of scientific research documents, whether they are published or not. The documents may come from teaching and research institutions in France or abroad, or from public or private research centers.

L'archive ouverte pluridisciplinaire **HAL**, est destinée au dépôt et à la diffusion de documents scientifiques de niveau recherche, publiés ou non, émanant des établissements d'enseignement et de recherche français ou étrangers, des laboratoires publics ou privés.



Distributed under a Creative Commons Attribution - NonCommercial 4.0 International License

(Zr/Ti) Ratio Effect On RF Magnetron Sputtered Lead Titanate Zirconate Films

C. SOYER, T. HACCART, E. CATTAN and D. REMIENS

LAMAC, Université de Valenciennes et du Hainaut-Cambrésis Z.I. du Champ del'Abbesse- 59600-Maubeuge-France

Sputtered $\text{Pb}(\text{Zr}_x\text{Ti}_{1-x})\text{O}_3$ thin films with various (Zr/Ti) compositions ranging from 15/85 to 70/30 were grown and characterised in terms of structural and electrical properties. PZT thin films, with 0.7–0.8 μm thickness, were deposited on Si/SiO₂/Ti/Pt by sputtering followed by conventional annealing. The sputtering conditions were the same for all the compositions. There were no apparent differences in crystallographic orientation as a function of Zr/Ti and the films a-lattice constant evolution is not exactly identical to the one of bulk ceramics. The permittivity increases when the Zr concentration increases and decreases just after the morphotropic composition i.e. Zr-rich films. The ferroelectric properties are very sensitive to the Zr/Ti ratio. For example, the coercive field increases when the Ti concentration in the film increases.

Keywords: $\text{Pb}(\text{Zr}_x\text{Ti}_{1-x})\text{O}_3$; various (Zr/Ti); rf sputtering; dielectric; ferroelectric

INTRODUCTION

Lead zirconate titanate thin films $\text{Pb}(\text{Zr}_x\text{Ti}_{1-x})\text{O}_3$ (namely PZT) is a widely studied ferroelectric material. Its interesting properties, dielectric, ferroelectric, pyroelectric [1,2] and piezoelectric [3,4], are attractive for numerous applications, such as ferroelectric memories and

micro-electro-mechanical systems (MEMs). For MEMs, PZT films must be thicker than those used in ferroelectric memories. When the film thickness increases from 0.3 to over 1 μm , dielectric, ferroelectric and piezoelectric properties are strongly modified and the main evolution has been reported to occur up to 1 μm [5]. For this purpose, a film thickness of about 0.8 μm has been chosen for the following study. The evolution of electrical properties with the chemical composition (i.e. Zr/Ti ratio) has been investigated currently in the frame of memory devices applications for films prepared either by sol-gel or MOCVD [6,7]. For sputtered films however, electric properties are usually reported for the morphotropic phase boundary (MPB) composition i.e. $x=0.54$. The influence of the Zr/Ti ratio is developed in only few papers [8].

The aim of this work is thus to study the evolution of structural, dielectric and ferroelectric properties of PZT films, with a higher thickness, in a wide range of chemical composition around the MPB. $\text{Pb}(\text{Zr}_x\text{Ti}_{1-x})\text{O}_3$ films, with a thickness of 0.8 μm and a Zr content ranging from $x=0.15$ to $x=0.7$, were performed by rf magnetron sputtering on Si/SiO₂/Ti/Pt substrates.

EXPERIMENTAL

PZT thin films were deposited by rf magnetron sputtering using a 3 inch diameter PZT target. This target was cold pressed powder, and the powder used was a stoichiometric mixture of single oxides. The Zr and Ti contents of the targets were altered to obtain PZT films of several compositions ($0.15 \leq x \leq 0.7$).

The results presented for PbTiO_3 ($x=0$) are coming from previous study [9].

The PZT films were deposited at room temperature and annealed at 625°C for 30 min to achieve a crystallised structure. The deposition and annealing conditions have been optimised for PZT films with $x=0.54$ and transferred to others compositions. They are summarised in Table 1. Si(100)/SiO₂/Ti/Pt(111) was used as substrates. The Titanium (200Å) and Platinum (1500Å) layers were deposited using rf sputtering on thermal oxidised silicon. Prior to depositing the PZT film, the Pt electrode was annealed at 650°C for one hour to enhance the adhesion of PZT to Pt and the nucleation of the perovskite phase.

TABLE 1 Sputtering deposition conditions of PZT thin films

Target diameter	76.2mm
RF power density	2.36W/cm ²
Target - substrate distance	60mm
Sputtering gas	Ar
Working gas pressure	30mTorr
Substrate temperature	25°C - 160°C

The crystal structure of the films was examined by x-ray diffraction. The microstructure of PZT thin films was studied using optical microscope (OM) and scanning electron microscope (SEM) and chemical composition was analysed by energy dispersion spectroscopy (EDS).

Pt top electrodes with diameter of 150 μ m and a thickness of 150 nm were obtained by photolithography and sputtering to form a Pt/PZT/Pt structure. Then, capacity and loss factor ($\tan\delta$) were performed using an impedance analyzer Hewlett Packard 4192A at a frequency of 10kHz and an alternative voltage $V_{AC}=100mV$. The ferroelectric loops (P-E) were measured using a Radiant RT6000 in a virtual ground mode.

RESULTS AND DISCUSSION

Structural properties

Figure 1(a) shows a OM surface morphology, whereas Figure 1(b) displays a cross section SEM microstructure of PZT (45/55) annealed thin film deposited on Si(100)/SiO₂/Ti/Pt(111) substrate. The OM surface morphology and cross section SEM microstructure obtained for samples with a different composition do not vary significantly. The morphologies of the films are crack free and uniform. These films consist of micron sized columnar dense grains with clear grain boundaries. No significant differences in the grain size or in the film density were noted between the films of various Zr/Ti ratios. A study by AFM is currently being conducted to observe more precisely the grains surface.

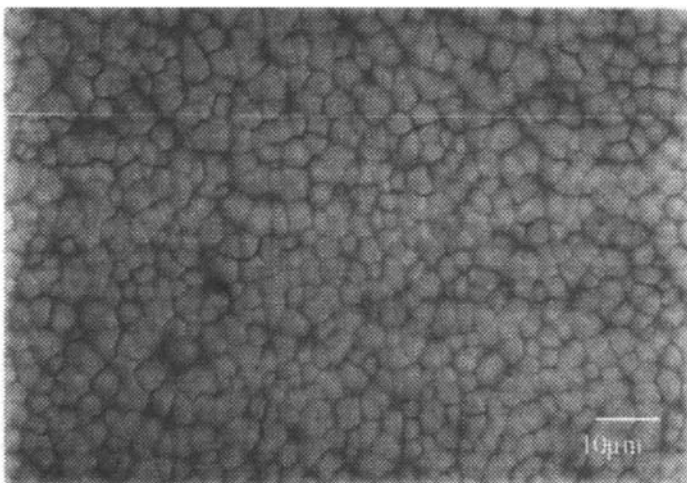


FIGURE 1(a) OM surface morphology of PZT(45/55) thin film. Surface morphology of PZT with different Zr content have the same aspect.

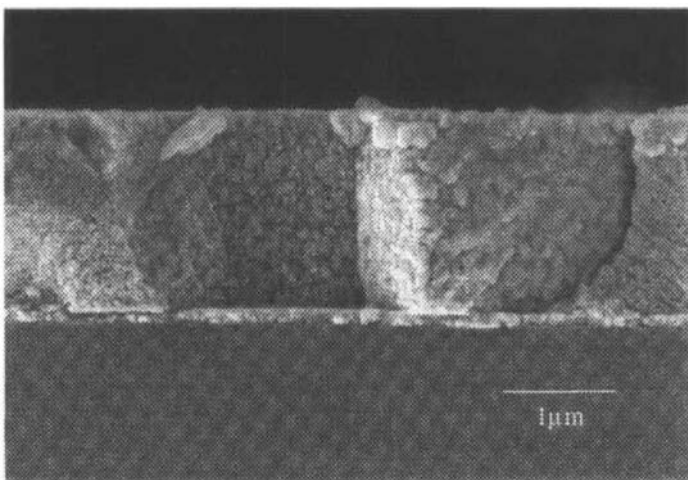


FIGURE 1(b) SEM cross-sectional view of PZT(45/55) thin film annealed at 625°C for 30min; substrate was Si(100)/SiO₂/Ti/Pt(111) and the film was 1.8 µm thick. However, the same microstructure is observed for thinner films.

In this study, whatever the ratio Zr/Ti, we have maintained the same sputtering conditions. These conditions were previously optimised for Zr/Ti = 54/46 [10]. The compositional changes of PZT films with sputtering parameters (gas pressure, rf power) were investigated. It was found that the Zr/Ti ratio remains relatively constant whereas the Pb/Zr+Ti ratio was clearly dependent of the sputtering conditions. So, using targets with various Zr and Ti contents does not require changing the sputtering parameters. The PZT films with different composition were analysed by EDS to control the real Pb, Zr and Ti contents in the films. We observed a good transfer between the targets composition and the films composition : the most important difference observed is around 6%, which is approximately the error of the measurement.

We also examined the crystalline structure evolution of PZT with $x=0.25, 0.35, 0.45$ and 0.54 as a function of the annealing temperature. The analysis was performed during the crystallisation annealing. The pattern obtained display that it's not necessary to change the annealing parameters. Therefore, x-ray diffractograms presented here were obtained after conventional annealing performed in the usual conditions (625°C for 30 min).

Pattern for thin films of PZT with Zr/Ti = 25/75, 30/70, 35/65, 45/55, 54/46 and 70/30 are shown in Figure 2.

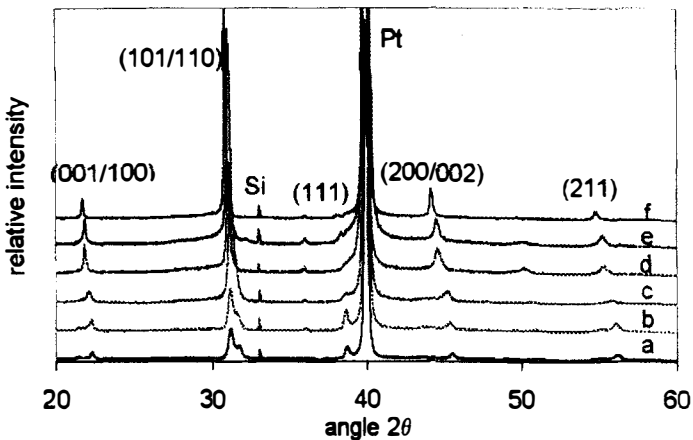


FIGURE 2 Evolution of XRD pattern for PZT films with various Zr content a) $x=0.25$, b) $x=0.30$, c) $x=0.35$, d) $x=0.45$, e) $x=0.54$ and f) $x=0.70$.

All the films exhibit a perovskite polycrystalline structure, without pyrochlore phase. Due to the various Zr/Ti ratios, changes in position of (100), (110), (111), (200) and (211) peaks of diffraction are observed. When $x \leq 0.30$, the diffractograms display split peaks for the (101/110) doublet, related to the tetragonal composition. When Zr/Ti = 35/65 and 45/65, a single peak is observed. This behaviour is in contradiction with result for bulk ceramics where the peaks splitting is systematically observed for Zr/Ti \leq 54/46.

The c/a tetragonality ratio, deduced from the doublet (001/100) for $x=0.15$ and $x=0.25$, was compared with reported c/a value for bulk ceramics of the same composition. This ratio is lower for thin films. Such a result has already been observed whatever the substrate nature for thin films performed by sol-gel [11], or for epitaxial PZT prepared by MOCVD [12]. As the tetragonal distortion is lower for thin films, the peaks splitting occurs for Ti-richer compositions.

The values of the lattice constant were determined from the diffraction angle related to (100) reflection. Figure 3 shows the evolution of a-axis lattice constant as a function of Zr content. The global trend is similar to that of bulk ceramics, but we have noted some differences. As already observed in literature [12,13], the a-axis lattice constant is larger than for bulk ceramics for tetragonal compositions, and smaller for rhombohedral materials. Moreover, the morphotropic phase boundary seems to be shifted to higher Ti content.

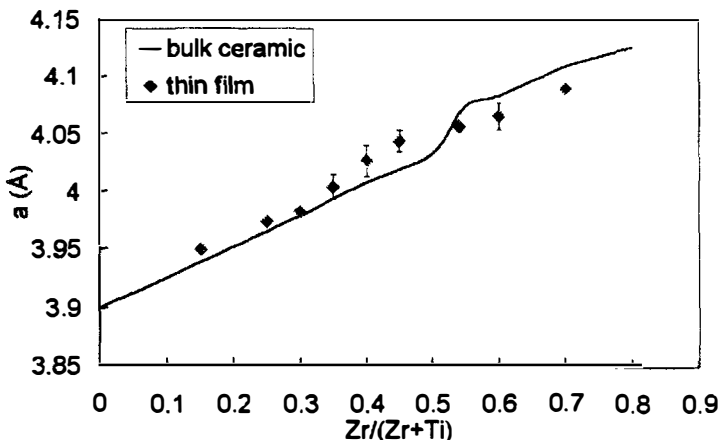


FIGURE 3 a-axis lattice constant as function of Zr content.

Dielectric properties

The value of relative dielectric constant ϵ_r was deduced from the capacitance. Figure 4 shows the evolution of ϵ_r as a function of the Zr/Ti ratio.

The maximum value ($\epsilon_r = 870$) was achieved near the morphotropic phase ($x=0.54$). This result is comparable to those reported for bulk ceramics [14], but the values obtained near the MPB remain higher for ceramics. This feature is also observed for PZT films grown by sol-gel [15,16] or MOCVD [17].

The dissipation factor $\tan\delta$ seems to be independent of the composition. Its value ranges from 1-3% whatever the Ti content.

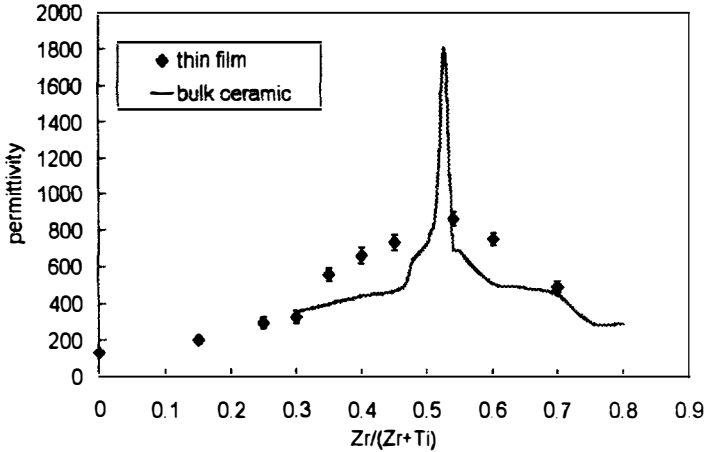


FIGURE 4 Permittivity ϵ_r as a function of Zr/Ti ratio

Ferroelectric properties

Different types of hysteresis loops were obtained with various Zr/Ti ratios : Zr/Ti=35/65 for the tetragonal phase, 54/46 for the MPB and 70/30 for the rhombohedral phase. These hysteresis loops are illustrated in figure 5. These three films were approximately $0.75 \mu\text{m}$ thick. For $x=0.35$, the hysteresis loop appears to be more squared, and exhibits a higher coercive field than for the MPB. The ratio Pr^+/Pm , with Pr^+ the remnant polarisation and Pm the maximum polarisation, is approximately equal to 0.64. By increasing the Zr/Ti ratio, Pr^+/Pm decreases. For $x=0.54$, Pr^+/Pm reaches 0.51 and the hysteresis loop is slimmer. Finally, for the rhombohedral composition, the ratio Pr^+/Pm is

still close to 0.5. Both remnant and maximum polarisations decrease and the hysteresis loop seems to be more tilted.

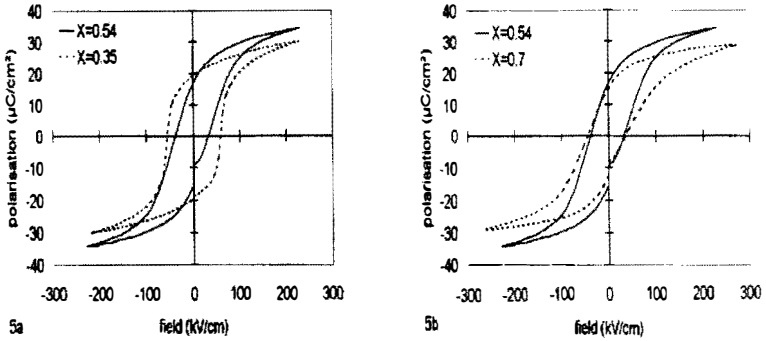


FIGURE 5 (P-E) hysteresis loop of PZT thin films with $x=0.35$, $x=0.54$ and $x=0.70$

Figure 6 shows the dependence of P_m and on the Zr/Ti ratio. It appears that the maximum P_m value is obtained at the MPB (P_m reaches $34 \mu\text{C}/\text{cm}^2$), but for Pr^+ , the best results seem to be obtained with a higher Ti content. Indeed, Pr^+ is equal to $20 \mu\text{C}/\text{cm}^2$ when $\text{Zr}/\text{Ti}=45/55$. Pr^+ values for $x=35/65$ and $40/60$ are also higher than the value for $x=54/46$.

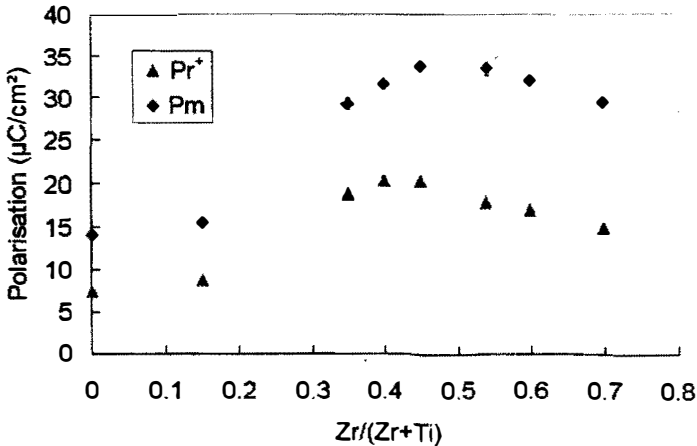


FIGURE 6 Maximum polarisation and remnant polarisation of $0.8 \mu\text{m}$ thick PZT thin films as a function of Zr content

Hysteresis loops are generally more square outside the MPB zone. The best piezoelectric properties can then be expected when the highest P_r^+ value is achieved, thus for a Zr/Ti ratio lower than 54/46.

The coercive field, determined by the hysteresis loop measurement, is an apparent coercive field. The average coercive field defined as $E_m = (|E_c^+| + |E_c^-|)/2$ is more representative. In Figure 7 we show the evolution of the average coercive field as function of the film composition. This curve displays clearly that increasing Ti content is linked to an increasing E_m . Pure $PbTiO_3$ is well known as a hard ferroelectric material with the highest E_m (150kV/cm) among the PZT film composition. For Zr/Ti ratio higher than $x=54/46$, E_m saturates and his value is around 38kV/cm. We do not observe as Lee et al [18] with sol gel films an increase of the average field for x superior to 0.55.

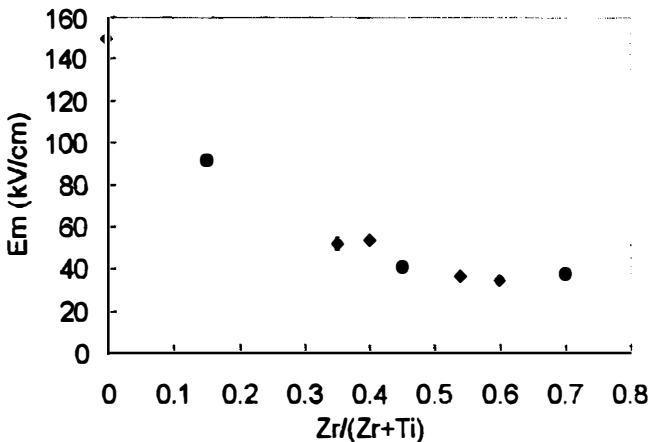


FIGURE 7 Variation of average coercive field E_m as a function of Zr content.

CONCLUSION

Thin films covering the full compositional range of $Pb(Zr_xTi_{1-x})O_3$, $0 < x < 0.8$ have been deposited by rf magnetron sputtering. We showed the systematic variations in the crystalline structure, dielectric and ferroelectric properties as a function of the composition. High values of remnant polarisation ($20\mu C/cm^2$) were observed at compositions around the MPB. Unlike previous studies, the dielectric constant exhibited a clear dependence on composition with values ranging from 120-870.

The coercive fields decreased with increasing Zr concentration to a minimum of 38kV/cm at the (60/40) composition.

These films, developed for applications integrating piezoelectric materials, as MEMs, are currently studied for their piezoelectric properties.

ACKNOWLEDGEMENTS

The use of facilities in Centre Régional de Transfert Technologique "Céramiques Fines" for samples analysis is gratefully acknowledged.

References

- [1] R. Bruchhaus, D. Pitzer, M. Schreiter, W. Wersing, *Journal of Electroceramics*, **3:2**, 151 (1999).
- [2] K.K. Deb, K.W. Bennett, P.S. Brody, B.M. Melnick, *Integrated Ferroelectrics*, **6**, 253 (1995).
- [3] K. Lefki, G.J.M. Dormans, *J. Apply. Phys.*, **76(3)**, 1764 (1994);.
- [4] M.A. Dubois, P. Muralt, *Sensors and Actuators*, **77**, 106 (1999).
- [5] R. Kurchania, S.J. Milne, *J. Mater. Res.*, **14**, 1852 (1999).
- [6] M. Shimizu, T. Shiosaki, *Mat. Res. Soc. Symp. Proc.*, **361**, 295, (1995).
- [7] A. Patel, E.A. Logan, R. Nicklin, N.B. Hasdell, R.W. Whatmore, U. Uren, *Mat. Res. Soc. Symp. Proc.*, **310**, (1993).
- [8] K. Lijima, N. Nagao, T. Takeuchi, I. Ueda, Y. Tomita, R. Takayama, *Mat. Res. Soc. Symp. Proc.*, **310**, 455 (1993).
- [9] D. Remiens, B. Jaber, P. ronc, B. Thierry, *J. Eur. Ceram. Soc.*, **16**, 467 (1996).
- [10] G. Vélú, D. Rémiens, B. Thierry, *J. Eur. Ceram. Soc.*, **17**, 1749 (1997).
- [11] N. Floquet, J. Hector, P. Gaucher, *J. Appl. Phys.*, **84**, 3815, (1998).
- [12] C.M. Foster, G-R. Bai, Z. Li, R. Jammy, L.A. Wills, R. Hiskes, *Mat. Res. Soc. Symp. Proc.*, **401**, 139 (1996).
- [13] T. Sakoda, K. Aoki, Y. Fukuda, *Jpn. J. Appl. Phys.*, **38**, 3600 (1999).
- [14] T. Yamamoto, *Jpn. J. Appl. Phys.*, **35**, 5104 (1996).
- [15] G. Teowee, F.S. Mc Carthy, B.H. Dietz, D.R. Uhlmann, *Integrated Ferroelectrics*, **22**, 431 (1998).
- [16] P. Muralt, M-A. Dubois, A. Seifert, D.V. Taylor, N. Ledermann, S. Hiboux, *Proceeding of ECAPD IV, Ferroelectrics*, **224**, 235 (1999).
- [17] M. de Keijser, P.J. Van Veldhoven, G.J.M. Dormans, *Mat. Res. Soc. Symp. Proc.*, **310**, 223 (1993).
- [18] E.G. Lee, D.J. Wouters, G. Willems, H.E. Maes, *Appl. Phys. Lett.*, **70**, 2404 (1997).